Postprint of: Castro-Muñoz R., Gontarek-Castro E., Karczewski J., Cabezas R., Merlet G., Araya-Lopez C., Boczkaj G., Hybrid cross-linked chitosan/protonated-proline:glucose DES membranes with superior pervaporation performance for ethanol dehydration, JOURNAL OF MOLECULAR LIQUIDS (2022), 119499, DOI: 10.1016/j.molliq.2022.119499

Hybrid cross-linked chitosan/protonated-proline:glucose DES membranes with superior pervaporation performance for ethanol dehydration

Roberto Castro-Muñoz[1,2*], Emilia Gontarek[3], Jakub Karczewski[4], René Cabezas[5], Gastón Merlet[6], Claudio Araya-Lopez[7], Grzegorz Boczkaj[1,8]

[1] Faculty of Civil and Environmental Engineering, Department of Sanitary Engineering, Gdansk University of Technology, 11/12 Narutowicza St., 80-233, Gdansk, Poland

[2] Tecnologico de Monterrey, Campus Toluca. Av. Eduardo Monroy Cárdenas 2000 San Antonio Buenavista, 50110, Toluca de Lerdo, Mexico.

[3] Faculty of Chemistry, Department of Process Engineering and Chemical Technology, Gdansk University of Technology, 11/12 Narutowicza St., 80-233, Gdansk, Poland

[4] Institute of Nanotechnology and Materials Engineering, Faculty of Applied Physics and Mathematics, Gdansk University of Technology, 11/12 Narutowicza St., 80-233, Gdansk, Poland

[5]Departamento de Química Ambiental, Facultad de Ciencias, Universidad Católica de la Santísima Concepción, Concepción, Chile

[6]Departamento de Agroindustrias, Facultad de Ingeniería Agrícola, Universidad de Concepción, Chillán, Chile

[7]Laboratory of Membrane Separation Processes (LabProSeM), Department of Chemical Engineering, University of Santiago de Chile, Av. Libertador Bernardo O'Higgins 3363, 9170022, Estación Central, Región Metropolitana, Chile

[8]Advanced Materials Center, Gdansk University of Technology, 11/12 Narutowicza St., 80-233, Gdansk, Poland

*E-mail: food.biotechnology88@gmail.com ; castromr@tec.mx (R. Castro-Munoz)

---

*Corresponding Author

Abstract

This work explores a protonated L-proline:glucose (molar ratio 5:1) deep eutectic solvent (DES) in fabricating biopolymer membranes utilizing chitosan (CS). Initially, the miscibility of CS and DES to prepare homogeneous dense blend membranes has been investigated. Different techniques, such as scanning electron microscopy, contact angle (CA), atomic force microscopy (AFM), Fourier transformed infrared spectroscopy (FTIR) and swelling degree (uptake), were used to characterize the structure of the resulting membranes. Within the pervaporation performance for ethanol dehydration, Arrhenius and mass transfer analysis were analysed in detail. Interestingly, the addition of DESs provided superior performance to crosslinked CS: DES membranes compared with the ones lacking DES. Based on the morphology and properties observed, this new concept of CS-based membranes can be alternatively applied in other solvent separations requiring hydrophilic membranes.

Keywords: Proline:glucose, deep eutectic solvents; chitosan; water-ethanol; hydrophilic pervaporation.

1. Introduction

A current trend of research deals with the implementation of deep eutectic solvents (DESs), which are an emerging class of sustainable solvents, into new applications and processes. Some examples of applications are as coatings [1], eco-friendly media in reactors [2], extraction of biomolecules from natural products, [3], separation of heavy metal from complex mixtures, CO_2 capture [4], fuel desulfurization [5], assisting chromatographic techniques [6], biodiesel synthesis aided with enzymes [7], chemical and biochemical reactions [8], among others. The importance of DESs relies on their non-toxic character, low cost in synthesis, easy to use, biodegradable, environmentally-safe and reusable [9]. As for DES synthesis, these eutectic mixtures tend to be typically formed by linking a hydrogen bond acceptor (HBA), usually quaternary ammonium salts, and a hydrogen bond donor (HBD) [1,10]. As for membrane fabrication, DESs are initially utilized as additive agents in DES-supported membranes [11,12], since they can confer a synergistic effect in the separation features of polymer membranes. In fact, such performance improvement showed by DESs in membranes is ascribed to a facilitated diffusion and adsorption of molecules within the functional groups present in DESs [13–15]. Apart from their application as additives, DESs were proposed as pore-forming additives in phase inversion process via immersion precipitation for synthesizing membranes with asymmetrical patterns [16].

Very recently, our research group has synthetized and implemented a new DESs, based on an amino acid and an organosulfur solute, for fabricating dense chitosan (CS) membranes, which were subsequently applied into the pervaporation (PV) separation of methanol/MTBE mixtures [17]. CS was proposed in this study since it is the most

investigated biopolymer for PV membranes with high performance for the removal of water molecules from less polar or non-polar molecules [18,19], e.g., CS has shown interesting permeation rates and salt rejection in seawater desalination via PV [20]. It is worth mentioning that biopolymer-based membranes (including CS, sodium alginate, cellulose acetate, polylactic acid, among others) are a current scope of study according to the need of replacing chemically synthesized polymers [21,22]. Apart from the implementation of DES in biopolymer membranes, the fabrication of mixed matrix membranes (or nanocomposites) through the incorporation of nanomaterials is also a current trend in the field [23–25]. Unfortunately, there is still a big need in finding new DES to assist the fabrication of polymer membranes and improve somehow their physicochemical properties and thus separation performance. It is worth mentioning that the main challenge comprises the rapport of the eutectic mixture and organic phase (i.e., polymer) towards their compelling joining. Here, in this research, an original hydrophilic eutectic mixture, like protonated L-proline:glucose at molar ratio 5:1, was used for the unprecedented tailoring of cross-linked CS membranes to beaten the typical issues associated with the suitable distribution of the eutectic mixtures inside the biopolymer.

Strategically, the new DES owning hydrophilic character and soluble in water, such as protonated-L-proline:glucose under optimized molar ratio 5:1, has been eventually elaborated [26]. After this, the DES was blended with CS phase to fabricate a homogeneous dope solution, succeeded by an *in-situ* cross-linking via glutaraldehyde (GA). These final membranes were fully characterized and evaluated for practical separation application. PV experiments towards the removal of water from azeotropic

92 water-ethanol model mixtures demonstrated the membranes' appropriateness. Finally, a
93 model based on the resistances-in-series model allowed us to characterize the mass
94 transfer phenomenon.
95
96 **2. Materials and methods**
97 *2.1. Chemicals and supplies*
98 As for L-proline, this has been acquired with a purity of at least 98% from Sigma Aldrich.
99 Glucose (pure, WarChem), hydrochloric acid (analytical reagent, POCH S.A.) and
100 glutaraldehyde (at 25 wt.% concentration) were obtained and utilized lacking in
101 additional treatment. The chitosan polymer has been purchased from Sigma Aldrich.
102
103 *2.2. Eutectic mixture preparation*
104 *A protonated-L-proline:glucose* (5:1) has been preliminarily prepared. Experimentally,
105 10 g of L-proline and 86.86 mL of HCl 1M were continuously blended at given
106 conditions (1000 rpm, 70 ℃) up to results in a homogenous and translucent mixture.
107 Next, glucose (3,13 g) was incorporated into the mixture. Residual water has been later
108 eliminated via evaporation (BUCHI Rotavapor R-300, V-300 vacuum pump).
109
110 *2.3. Membrane fabrication*
111 Overall protocol for membrane preparation is graphically described in **Figure 1**. All
112 chitosan-based membranes have been fabricated using dense-film casting method. To
113 formulate the dope solutions, the right quantity of CS (1.5 wt.%) was dissolved in 2 wt.%
114 acetic acid in water. The polymeric dope mixtures were kept in agitation during a day.

After that, eutectic mixture L-proline:glucose (5 wt.%) has been then incorporated in dope mixtures. Importantly, 5 wt.% of eutectic mixture corresponds to the best ratio for the membranes, agreeing with previous studies [17,27]. The final solution was mixed during 4 h before the application of the *in-situ* cross-linking with GA, which was initially applied to confer a better chemical and solvent stability of the membranes, while ensuring the DES restraint into the polymer membrane [28]. The *in-situ* cross-linking has been performed using GA (100 µL), followed by HCl (100 µL). This final mixture was homogenized during 15 min, and then cast. Membrane samples were subjected to drying at 25 ℃ over 2 days. In general, the membranes' physical aspect has been found as typical homogeneous and continuous film phase with a thickness ca. 25 µm. Finally, the final membranes were named as follows: cross-linked CS & cross-linked CS:L-proline:glucose, labelled as CS:PRO:GLU.

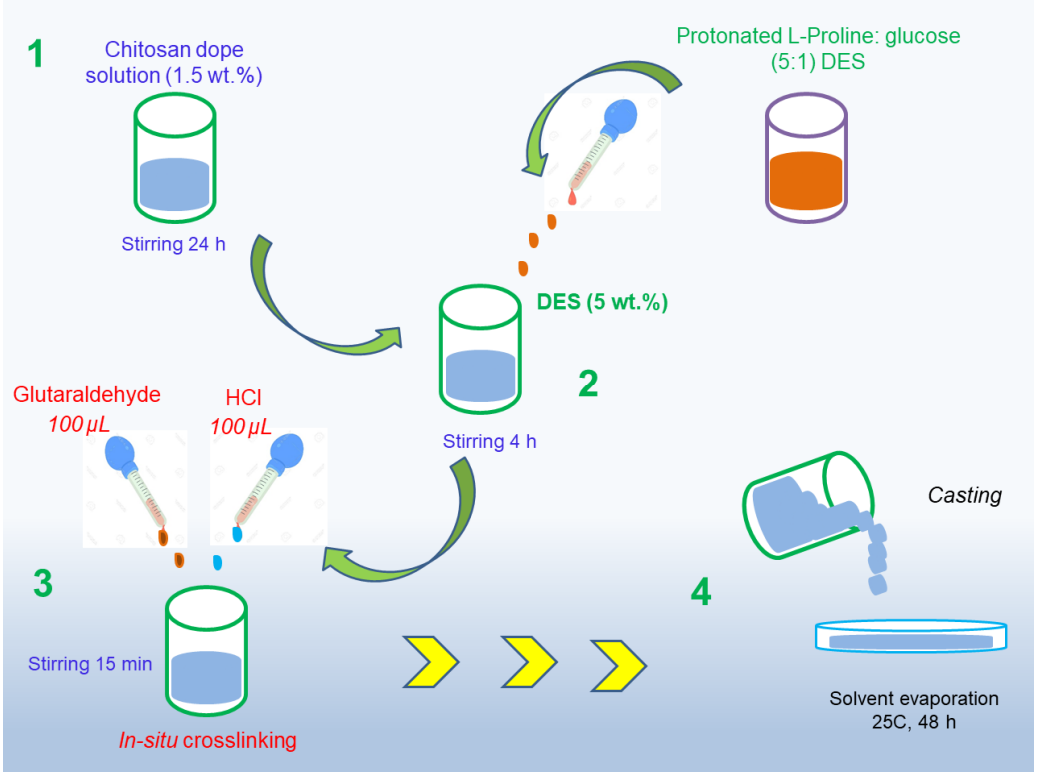

Figure 1. Preparation strategy of crosslinked chitosan membranes containing L-proline: glucose eutectic mixture.

2.4. Membrane analysis and characterization

Microscopy techniques: SEM and AFM: Structure-morphological property was studied via FEI Quanta FEG 250 SEM microscope. The secondary electron detector was also utilized for the investigation, recording micrographs (at 5 kV accelerating voltage) in high vacuum mode. Preliminarily, the membrane samples were essentially coated via sputtering (gold layer ca. 10 nm), which was applied to balance the scares surface conductivity. The respective micrographs were obtained at proper magnification. Regarding cross-section, membrane specimens were fractured by immersing in liquid N_2. On the other hand, AFM studies were done using Nanosurf EasyScan 2 by contact mode using silicon tips (AppNano - SICON series) with 10nN constant force [29].

FTIR analysis: Membrane samples have been analysed via Nicolet iS10 spectrometer (from Thermo Fisher Scientific) presenting deuterated triglycine sulfate (DTGS) detector, along with a Golden Gate diamond ATR. Under resolution of 16 cm^{-1}, spectra data was acquired in the range 4000–400 cm^{-1}.

Contact angle determination: The surface CA determination has been done with ultrapure water. In this analysis, goniometer OCA15 (Data Physics) was utilized. The data were reported as the average and standard deviation (SD) of at least five assays.

2.4.1. Uptake: As for solvent uptake, which gives the solvent adsorption ability [30], has been investigated for pure ethanol and different water-ethanol mixtures ranging from 0-50 wt.% water in ethanol. Membrane sample (approximately 1×5 cm) was first weighed;

after this, it was then subjected to immersion in the binary solvent mixtures (at room temperature, 2 days). As documented in other investigations [31], the wet membrane pieces need to be fast cleaned to eliminate the possible residual solvent from surface. Right away, the weight of the samples was again determined (digital balance, Gibertini, Crystal 500, Italy). The uptake calculation was done accordingly [32]:

$$Uptake\ (\%) = \frac{W_f - W_i}{W_f} \cdot 100 \qquad \text{Eq. (1)}$$

where W_f and W_i are the weight values for wet samples after immersion and dry before immersion, respectively.

2.5. Pervaporation separation performance

PV tests have been done in a lab operation unit; the schematic illustration and additional information are observed in previous works [33]. In general, an azeotropic water-ethanol (10–90 wt.%, respectively) mixture was poured into a PV cell. The solvent temperature was controlled (20, 30, 40 and 50 ℃) and kept constant utilizing a thermo digital circulating bath. At permeate side, the vacuum pressure was controlled at 1 mbar via CRVpro 4 vacuum pump (Welch Vacuum Products, USA).

Membrane samples with an active area of 5.3 cm^2 were located on a porous metal support at PV cell. Experimentally, permeating vapour was simultaneously condensed and collected by means of glass trap located inside a condenser containing liquid nitrogen. When steady-state was observed, the permeate samples were obtained from for 4 h running test and right away weighted to estimate the total permeate flux (J):

$$J = \frac{Q}{A \cdot t} \qquad \text{Eq. (2)}$$

where *Q* belong to the weight of the permeate (expressed in kg), *A* is the active membrane area (m^2) while *t* is the testing time (h). The partial flux (J_i) has been evaluated as the product of its respective weight fraction (y_i) accordingly [34]:

$$J_i = Y_i \cdot J \qquad \text{Eq. (3)}$$

The separation factor (α) was estimated as follows [34]:

$$\alpha = \frac{y_{water}/y_{ethanol}}{x_{water}/x_{ethanol}} \qquad \text{Eq. (4)}$$

where *y* and *x* belong to the weight fraction of each compound present in permeate and feed, respectively. The permeate samples composition was analyzed using Autosystem XL gas chromatograph with flame ionisation detector (FID) and split/splitless injector (Perkin Elmer, USA). Separation was done using a 60,0 m x 0,32 mm ID x 1 um (DB-624) capillary column (Agilent, USA).

The *J* and *α* data were given as the average of at least three tests to guarantee the results' accuracy.

2.6. Mass transfer analysis

To understand the mass transfer in the pervaporation system, the resistances-in-series theory has been used based on the solution-diffusion mechanism [35]. Considering the solution-diffusion model, a mass transfer flux of a component i can be denoted as a function of an overall mass transfer coefficient and a driving force, as follows:

$$J_i = K_{overall,i}(P_i^{\circ}\gamma_i x_i - P_P y_i) \qquad \text{Eq. (5)}$$

Where, $K_{overall,i}$ denotes the total mass transfer coefficient for the component i, P_i° is the

vapour pressure for the component i, γ_i is the activity coefficient of the component i, P_P is the total pressure at the permeate side, x_i is the molar fraction of the component i at the liquid side, and y_i is the molar fraction of the component i at permeate side. In a pervaporation system, the permeate side is under vacuum pressure so that the total pressure at the permeate side can be neglected, and Eq. (5) can be rewritten and simplified as follows:

$$J_i = K_{overall,i} \cdot (P_i^{\circ} \cdot \gamma_i \cdot x_i) \quad \text{Eq. (6)}$$

According to García et al. [36] and Arregoitia-Sarabia et. al. [35], overall mass transfer coefficient can be described as the combination for individual resistances

$$\frac{1}{K_{overall,i}} = \frac{1}{K_{l,i}} + \frac{1}{K_{m,i}} = \frac{P_i^{sat}\gamma_i}{k_{L,i}\rho} + \frac{\delta}{P_i} \quad \text{Eq. (7)}$$

where $k_{L,i}$ is the mass transfer coefficient for the component i at the liquid side, ρ is the density of the liquid feed, δ is the membrane thickness, and P_i is the permeability of the membrane for the component i.

The mass transfer coefficient has been calculated using the following correlation based on the work of Johnson et. al. [37]:

$$Sh = \frac{k_{L,i} \cdot d_{pervaporation\ cell}}{D_{sol}} = 0{,}0924 \cdot \left[\frac{\mu}{\rho \cdot D_{AB}}\right]^{0,5} \cdot \left[\frac{R \cdot d^2 \cdot \rho}{\mu}\right]^{0,71} \quad \text{Eq. (8)}$$

where $d_{pervaporation\ cell}$ is the diameter of pervaporation vessel, D_{AB} represents the diffusion coefficient, μ regards the viscosity of the mixture, d is the diameter of propeller, and R is the revolution per second of the propeller.

Finally, the membrane selectivity ($S_{i,j}$) and pervaporation separation index (PSI) are determined as follow:

$$S_{i,j} = \frac{P_i}{P_j} \quad \text{Eq. (9)}$$

$$PSI = J(S_{i,j} - 1) \quad \text{Eq. (10)}$$

3. Results and discussion

3.1. *Structure-morphological analysis.*

As for prepared membranes either with/without DES, they exhibited a convincing flat and smoothie surface with no apparent defects. It was visibly clear that there is no sign of being plastically deformed, this latter is characteristic of dense polymeric membranes [38]. For pristine CS membrane, cross-section view (**Figure 2b**) showed clear crater-like structure. This is typically observed when deforming via freeze-fracture. Additionally, this typical structure has been also observed in other pristine biopolymer membranes (like chitosan) [28,39]. Referring to CS:PRO:GLU membrane (**Figure 2d**), it also showed a homogeneous dense structure lacking in pores or pinholes between the organic phase and eutectic mixture. Essentially, the obtained morphology is considered as convincing proof of exceptional blending/miscibility among the hydrophilic eutectic mixture and CS, this has been reported in precedented studies, e.g., in polymer/polyethylene glycol blend membranes [40,41].

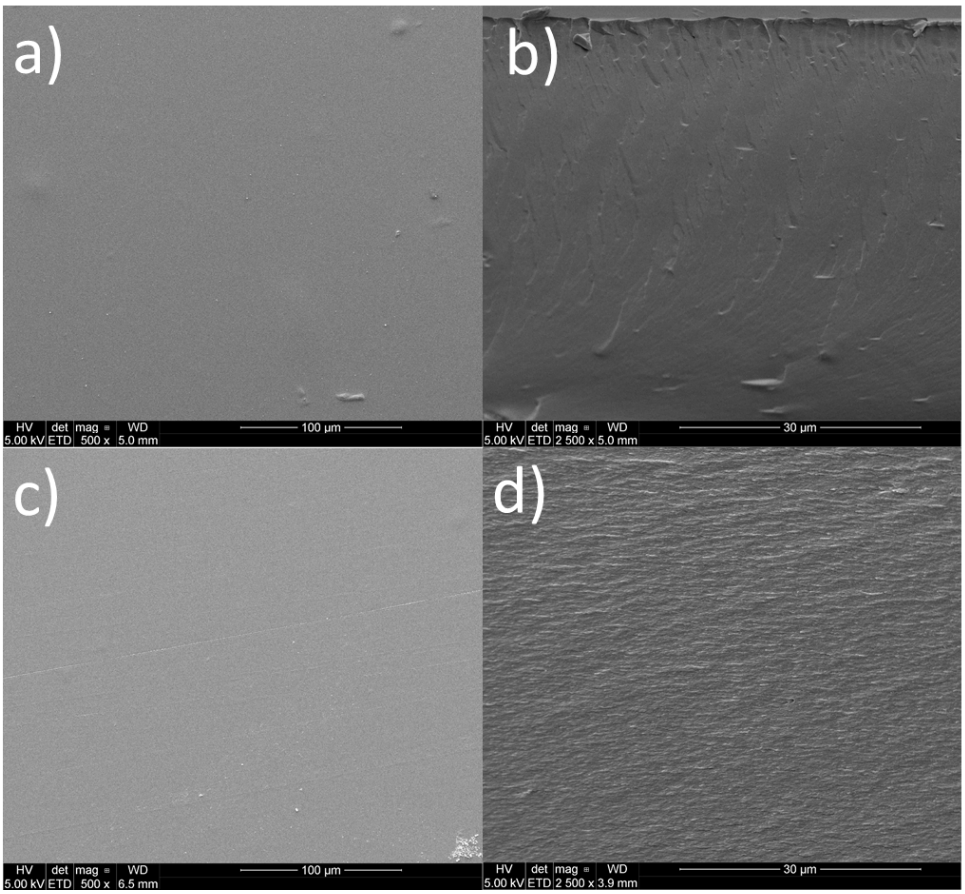

Figure 2. SEM surface and cross-section micrographs of the fabricated CS and L-proline:glucose membranes. (a, b) cross-linked chitosan and (c, d) cross-linked chitosan:L-proline:glucose (CS:PRO:GLU).

Herein, the incorporation of this eutectic mixture has interestingly contributed to obtain a compact but less smooth morphology. As mentioned previously, it has been documented that DESs can act as pore former additive to prepare of porous membranes [16,42]. In this case, our scope is proposed to physically merge and enmesh the chosen hydrophilic solvent in the hybrid membrane for potentialize its separation effect once maintained in the membrane structure. Our hypothesis relies on

245 the tremendously success of DESs for the extraction of low molecular weight molecules
246 based on their property to tremendously generate H-bonds by means of dipole-dipole
247 and coulombic forces, among other solute-solvent complexing synergy [43,44].
248 The eventual success of obtaining homogeneous dense membranes, with convincing
249 evidence of non-DES encapsulation, is due to the synergy of CS at linking some agents
250 thanks to its functional groups. In other words, the lack of functional groups among both
251 phases (i.e., polymer and DES) will consequently lead to not enough interacting
252 properties and consequently minimal miscible features [45]. These latter properties
253 become relevant when dealing with the merging of inorganic/organic dispersing agents
254 into polymers, where potential presence of functional groups or chemically
255 functionalized nanosized materials eventually achieves good synergy and contact at the
256 interface among polymer and filler [46].
257 CS itself presents a large number of NH_2 and OH terminal domains, which makes the
258 biopolymer an exceptional polymer for polymer blend formation [19]. While specific
259 DESs should also possess functional groups to synergistically interact with CS
260 conferring specific properties to the final membrane. Here, it is quite possible that this
261 hydrophilic DES (PRO: GLU), presenting various functional groups (e.g., amino,
262 hydroxyl, oxygen and carbonyl containing groups), could interconnect with CS. Clearly,
263 the surface micrograph of the blend membranes proves a smooth, continuous and
264 defect-free surfaces with lack of any pinholes. In literature, other DES, such as choline
265 chloride-malonic acid, was able to turn the flat surface of chitosan films to a non-
266 homogenous morphology while keeping a compact pattern [47]. In this study, we also
267 confirm a smoother surface by adding the DES agent into CS, as observed in **Figure 3**.

It is worth mentioning that the DES-free crosslinked CS membrane displayed an average root mean square roughness of S_q=4.0±0.5 nm, where the incorporation of DES slightly lowered such value to S_q=3.0±0.5 nm. Certainly, upon the nature of the eutectic mixture, the exaggerated load of the DES may promote a rough structure of the final eutectic-chitosan blend membranes [48].

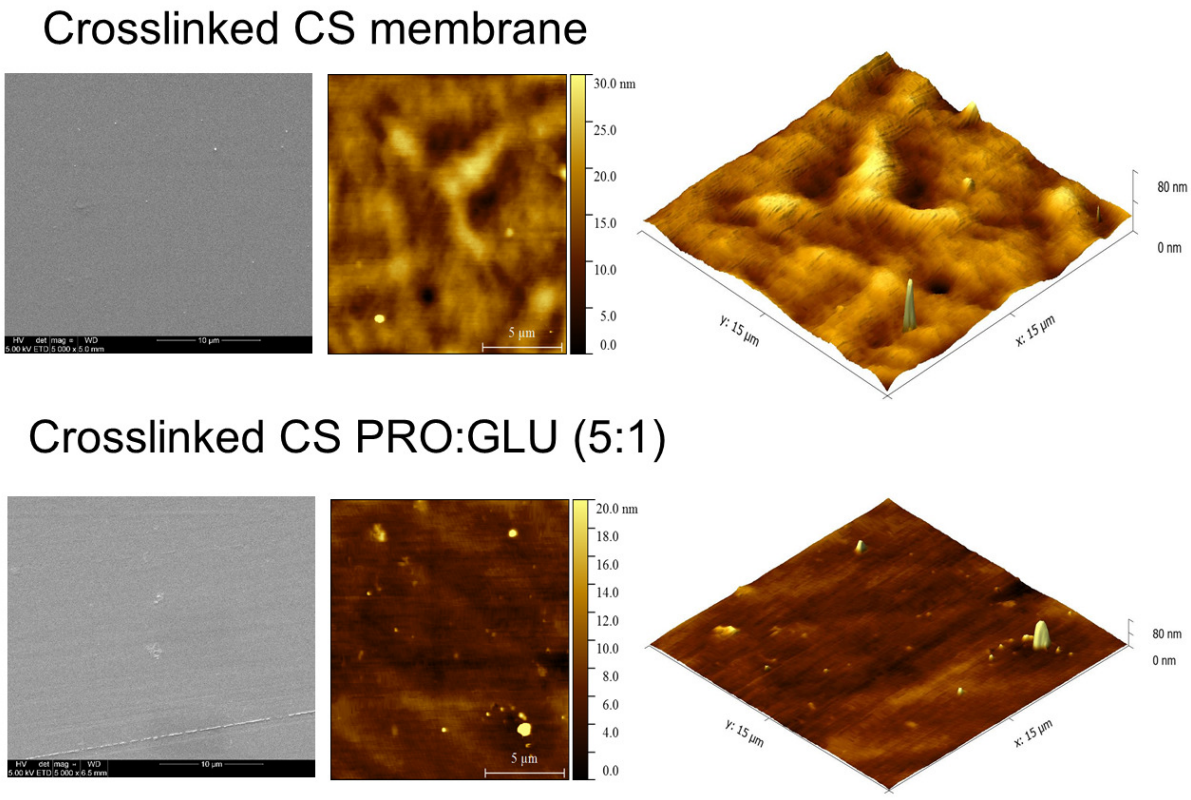

Figure 3. AFM surface and 3D images (15 × 15 µm) of pristine CS and CS:PRO:GLU membranes.

It is worth mentioning that the blending of DES into CS membrane may influence the mechanical and thermal properties of the resultant membranes. In a previous work, it has been stated that eutectic mixtures (e.g., based on L-proline:sulfolane) worsened specific mechanical properties, such as Young's modulus and tensile strength, but such

an effect was compensate due to the *in situ* cross-linking [17]. DESs tend to decrease the intermolecular interactions in the CS network, causing the co-called plasticization. The incorporation of plasticizers (like DES) in CS, in fact, produces a transition from a rigid to a softer material with elastic properties [49]. Aside from this effect, DES has been demonstrated to affect the thermal stability of the CS membranes in terms of glass transition temperature (T_g), e.g., DES-modified CS films exhibited a lower T_g in comparison with bare CS membranes. Eventually, this can be ascribed to eutectic mixture decomposition. Interestingly, T_g values decreased proportionally as the DES content increased. According to Jakubowska et al. [47], DES concentration increment results in a decrease in temperature at which decomposition starts.

3.2. *FTIR and water CA characterization*

As seen in **Figure 4**, the FTIR data essentially confirms the effective merging of the hydrophilic PRO:GLU solvent and the biopolymeric phase. Full spectrum data show a firm and vast patterning with asymmetry ranged approximately 3350-3450 cm^{-1}, which a consequence of overlaying the O-H and N-H stretching oscillations of terminal groups connected by H-bonds. Typically, CS spectrum exhibits a various absorption patterns around 1650 cm^{-1} (which corresponds to C=O stretching of possible $CO=NH_2$ terminal group), 1520 cm^{-1} (which corresponds to N-H wagging of non-acetylated 2-aminoglucose) and ca. 1580 cm^{-1} (which corresponds to N-H wagging of $CO=NH_2$ terminal), which evidenced by other reports [50]. Apart from that, absorption patterning located ~ 1150 cm^{-1} refer to a skew-symmetric stretching for C-O-C links, 1060 cm^{-1} and 1050 cm^{-1}, ascribed to possibly skeletal frequencies comprising a typical C-O

303 conjunction. Concerning to the DES, the amino acid (L-proline) owns an extra -NH_2
304 terminal, identified as an RR'C=NR". Hence, proline is also identified as an imino acid.
305 As proline's three-carbon R-grouping tends to be merged to the alpha-nitrogen terminal,
306 this molecule presents a restrained rigid-ring with rotational behaviour [26]. In the case
307 of glucose, it is a monosaccharide presenting six carbon atoms and an aldehyde group.
308 Considering the typical structure of any DES, both molecules (HBA and HBD) are
309 structurally well attached via electrostatic interaction (i.e., H-bonds) to form a final
310 eutectic system [51], this latter interaction is apparently observable with a firm shifting
311 and oscillation for the peak ranged from 3750-1950 cm^{-1} [52]. When this PRO:GLU
312 eutectic system is fused in the CS, this results in modest but clear motion on the usual
313 polymer patterning. This latter interaction reveals an exceptional attraction between
314 phases and is translated to affinity. Clear motions, together with the classic behaviour of
315 the patterning, in the range of 3650- 3100 cm^{-1}, must also be noted showing an
316 overlying of the spectra, which are ascribed to O–H, N–H and C—O oscillations in
317 chemical functionalities of the eutectic mixture and polymer. Jakubowska et al. [47]
318 have also reported similar molecular interactions when prepared and characterized
319 chitosan/DES hybrid materials. Importantly, the resulting reticulated flat films containing
320 glutaraldehyde commonly demonstrate clear absorption increment among 1600-1650
321 cm^{-1} thanks to N=C bonds [53,54]. The widening at 1550, 1740 and 2850 cm^{-1} refers to
322 the free aldehyde chain and raised C-H length, respectively. Aliphatic -NH_2 terminals
323 decay directly proportional as the peak 1150 cm^{-1} decreases. Alternatively, DES have
324 been identified as potential cross-linker agents for CS. Especially, eutectic mixtures
325 containing carboxyl groups are able to interact with the NH_2 groups of CS creating an

amide connection [48]. Such an amide connection has been also been observed in CS membranes blended with choline chloride -citric acid [52]. Interestingly, the blending of choline chloride-urea DES into the CS structure was able to create the saccharide ring (C–O–C) between DES and CS, proving the formation of a resilient solid biopolymer membrane without adding cross-linking mediator [55].

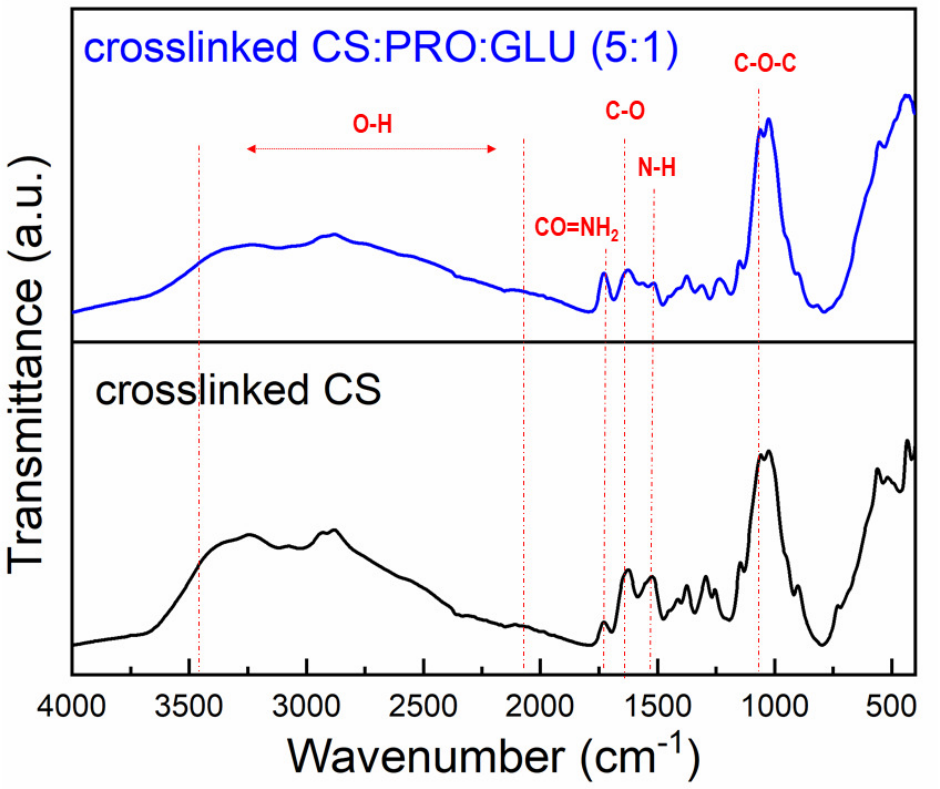

Figure 4. Spectrum data from FTIR measurement for pristine crosslinked chitosan and its eutectic mixture-based blend membrane.

A relevant point to highlight during the addition of this hydrophilic DES in membranes

regards its remarkable response on either hydrophilic or hydrophobic nature of the membrane. The DES-free cross-linked chitosan flat membrane revealed angle values of ca. 70° (see **Figure 5**), which agrees with outcomes published previously, e.g., angle values of chitosan nearly 74-88° [50,56]. In principle, the nature (either hydrophilic or hydrophobic) of the biopolymer indeed stands on its degree of deacetylation, e.g., large deacetylation gives as a result exceptional hydrophilicity in membranes due to many NH_2 terminals tend to be available in the biopolymer [57], this becomes relevant since hydrophilicity is needed for enhanced water adsorption over a membrane interface [58]. Hydrophilic nature of chitosan follows from its polar hydrophilic terminals, including -NH_2 and -OH; unfortunately, this polar nature is compromised when applying cross-linking. However, the addition of the PRO: GLU DES in the CS contributed to an enhanced hydrophilicity translated to lower CA values of ca. 50°. This gives an idea that the polar groups given by the DES have a meaningful influence at improving the hydrophilic nature of the membrane. Importantly, glucose is classified as polar since hydroxyl groups presents high affinity to hydrogen bonds and effective electronegativity.

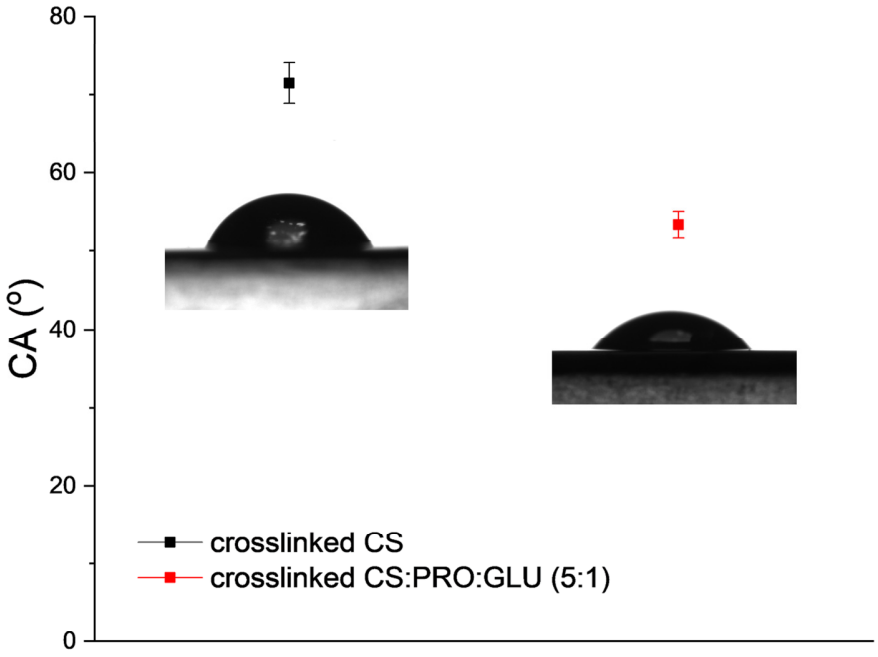

359

360

361 **Figure 5.** CA values pristine crosslinked CS and CS:PRO: GLU membranes.

362

363 3.3. *Pervaporation testing*

364 *3.3.1. Operating temperature dependence of permeation and separation factor.*

365 PV data for all assayed membranes are reported in **Table S1**. **Figure 6** shows the
366 influence of the feed temperature on the total permeation flux, in which a permeation
367 increase was noted in the range of 20-50 ℃ in pristine cross-linked and its blend with
368 PRO: GLU DES. It is actually traditional behaviour for polymers as their chains tend to
369 present improved flexibility under high temperature, which consequently contribute to
370 enhanced solvents' sorption. This consequently increases the transport of molecules

371 across the intermolecular distances of polymer membranes [59].

372

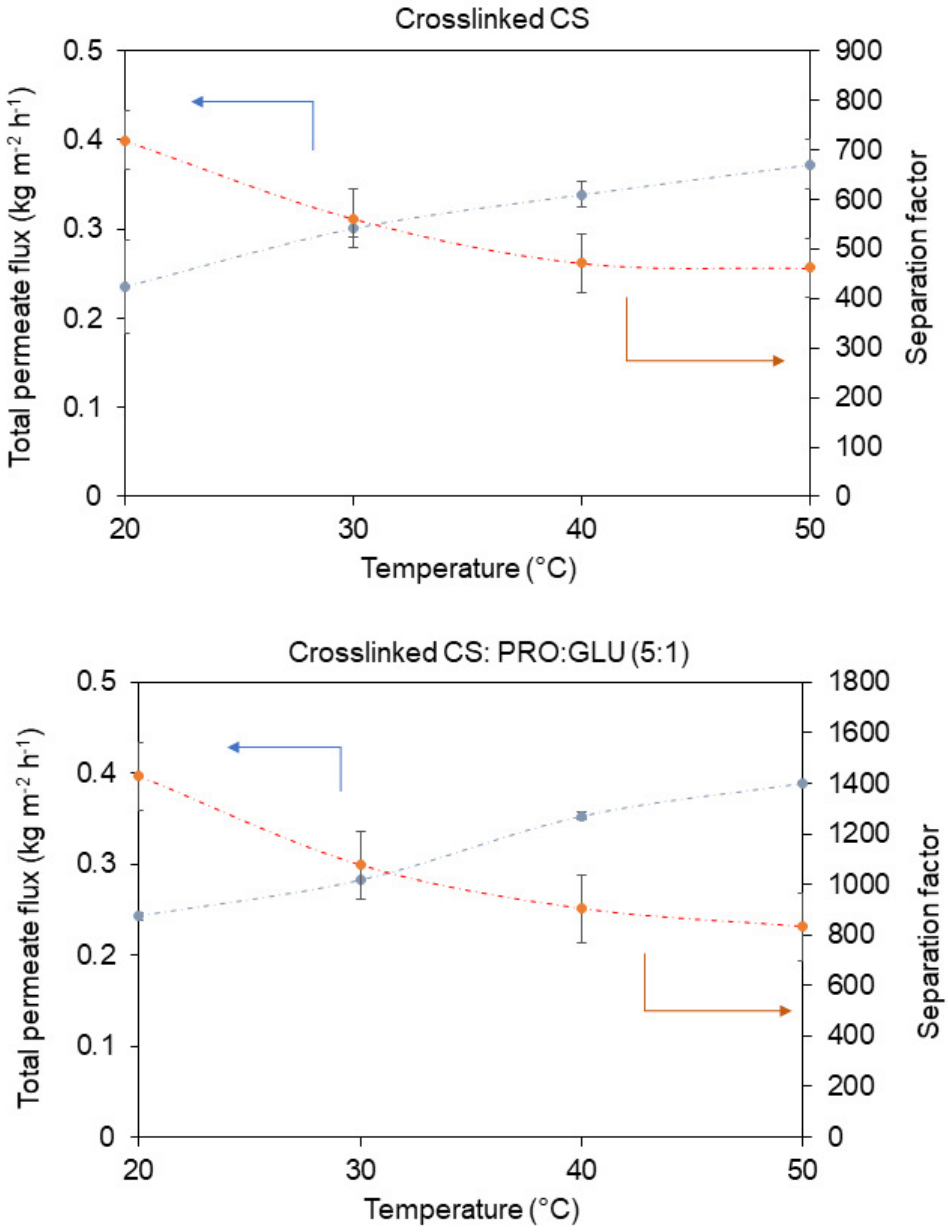

373

374 **Figure 6.** Permeation and separation factor behaviour in respect to operating

375 temperature (10/90 wt.% H_2O/EtOH, pressure: 1 mbar). The semi continuous loops are

376 only guiding.

Essentially, an influence of temperature on overall flux was further analysed by means of the Arrhenius equation, as denoted in Eq. 11.

$$J = J_o \cdot \exp\left(-\frac{E_{app}}{R \cdot T}\right) \qquad \text{Eq. (11)}$$

In theory, J_o refers to the pre-exponential element, while E_{app} corresponds to the apparent activation energy for the transport. The product $R \cdot T$ expresses the typical term of energy. By applying mathematical logarithms in previous Eq. (11), E_{app} is determined directly from the straight line proving a compelling relationship between flux and temperature; it means, an increment in overall flux occurs with temperature increase. As **Table 1** reports, it is noted that water displays lower E_{app} values (ca. 5.07 kJ mol^{-1}) in respect to ethanol (~10.27 kJ mol^{-1}) in crosslinked CS membrane, confirming the water affinity of chitosan. On the other hand, the eutectic solvent blending slightly increased the E_{app} in water molecules approximately 5.57 kJ mol^{-1} for the hybrid CS:PRO:GLU membrane, however, E_{app} value for ethanol has been more impacted by DES incorporation. Particularly, the E_{app} keeps unchanged towards water in respect to ethanol ranging from 20 to 50 ℃. It is important to point out that the temperature increment impact mainly the water permeation, and it is greatly restricted the permeating ethanol; this is supported by Almeida et al. [60], who documented an improved water solubility in CS films containing DES, in which the water solubility increased when increasing the DES content. In this study, the existence of this hydrophilic PRO: GLU increases the energy demanded for the

permeating solvent to be transported over the membrane interface, which is more prominent for ethanol. This latter aspect is in agreement with the DES hydrophilicity, which favours for the selective properties for the more polar compounds (like water) [61].

Table 1. Apparent activation energy values for overall flux, and single water and ethanol across prepared hybrid materials.

Hybrid formulation	E_{app} **(kJ mol^{-1})**		
	Overall	Water	Ethanol
Crosslinked chitosan	5.15	5.07	10.27
Crosslinked CS:PRO:GLU	5.63	5.57	11.76

When dealing with selective affinity, α parameter in pure CS membrane decayed when the temperature decreased, as seen in **Figure 6**. Promisingly, separation factor was substantially enhanced via DES incorporation observing data of ca. 1,427 (at 20 ℃). Obviously, large α parameters with lower permeating yield were indeed recorded at the minimal testing temperature. It somehow in accordance to the polymer "free-volume" theory, as it declares a thermal movement in chains specifically at amorphous localities boosting an increment in free-volume. It is known that as temperature raises, the frequency and magnitude of the chain swing increases provoking a free volume increment [62]. Although the kinetic diameters of water and ethanol are substantially different (2.6 and 4.3 Armstrong, respectively), the thermal movement in polymer chains

417 can indeed facilitate the diffusivity for bigger solvent molecules (like ethanol) over a
418 membrane interface compromising the separation factor. In addition to this, hydrophilic
419 eutectic mixtures have demonstrated to break the intermolecular structure of CS and
420 thus open the network structure, allowing the permeation of solvent molecules [48,60].

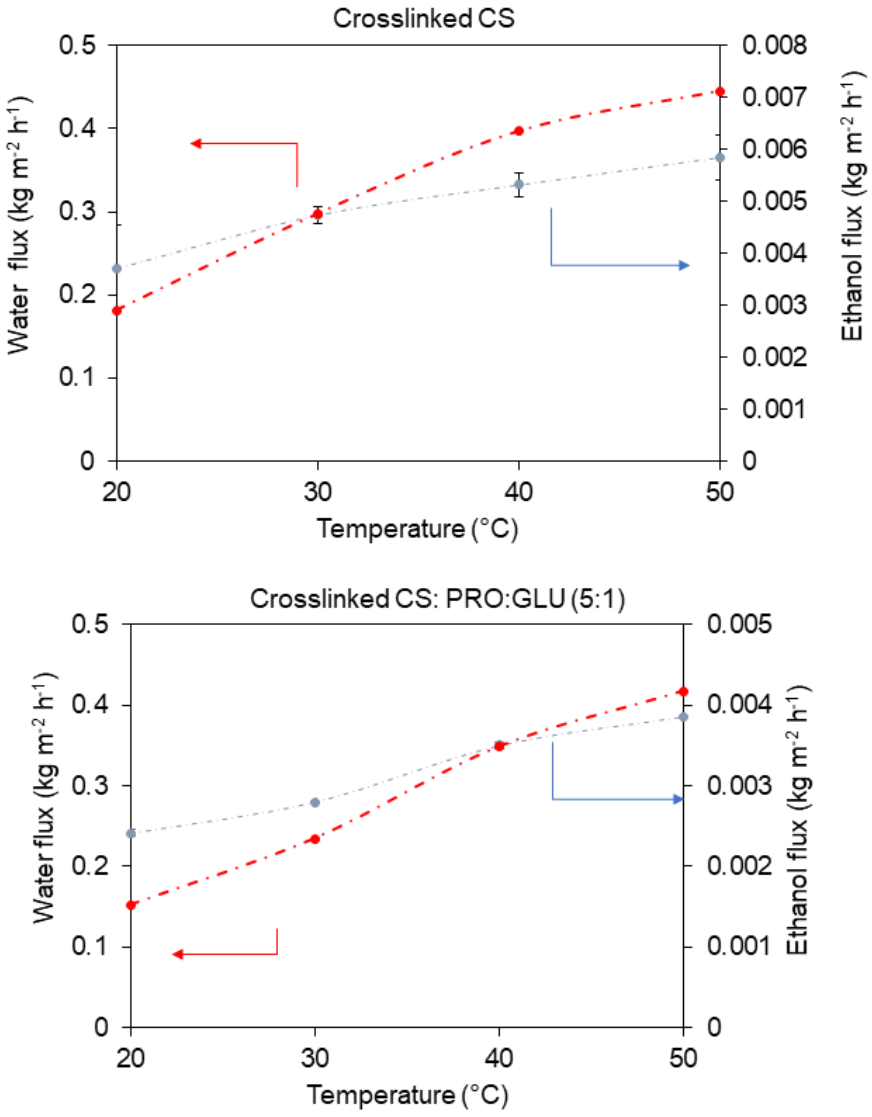

421

422 **Figure 7.** Water and ethanol flux in respect to operating temperature (10/90 wt.%
423 H_2O/EtOH). The semi continuous loops are only guiding.

424

425 Very recently, Jakubowska et al. [47] have reported that the DES addition promotes the
426 free volume increment in polymeric matrices. This is ascribed to the enlargement of
427 free-volume fostering the chain motion, which can produce a decrement for the
428 membrane's selective efficiency. However, an application regarding this hydrophilic
429 PRO: GLU DES did not affect the selective properties of CS membrane. Interestingly,
430 both parameters, such as permeation rate and selectivity, were significantly improved.
431 As shown in **Figure 7**, DES preferentially promoted the passage of water molecules
432 over the polymeric phase while concurrently hindering a possible ethanol permeation. At
433 this point, the polarity of the solvents becomes relevant for their own transport and
434 extraction from complex systems [63].
435 The analysis for the solvent uptake in the developed membranes is represented in
436 **Figure 8**. It is clearly observed how both membranes show low solvent uptake when
437 there is a minimal concentration of water in the ethanolic solutions. Experimentally, a
438 water concentration increment of the feeding solvent mixture resulted in a higher
439 membrane swelling in a water concentration from 10 to 50 wt.%. Surprisingly, the
440 incorporation of PRO: GLU DES provoked a decrement in terms of solvent uptake
441 performance compared with the pristine CS. This latter phenomenon supports
442 Jakubowska's findings [47] in which a DES confers stability in chitosan membranes.
443 The uptake is generally expected to be restricted once a crosslinking protocol is
444 implemented as this treatment provides resistance to polymer materials against polar
445 solvents thanks to an enhanced stricture in mobility of chains [64]. Swelling
446 phenomenon is adequately identified as one of the primary bottlenecks of hydrophilic-
447 based polymer materials when separating polar molecules [20]. Therefore, less prone to

448 be swollen membranes are preferentially needed to acquire a stable separation during
449 long-term testing.

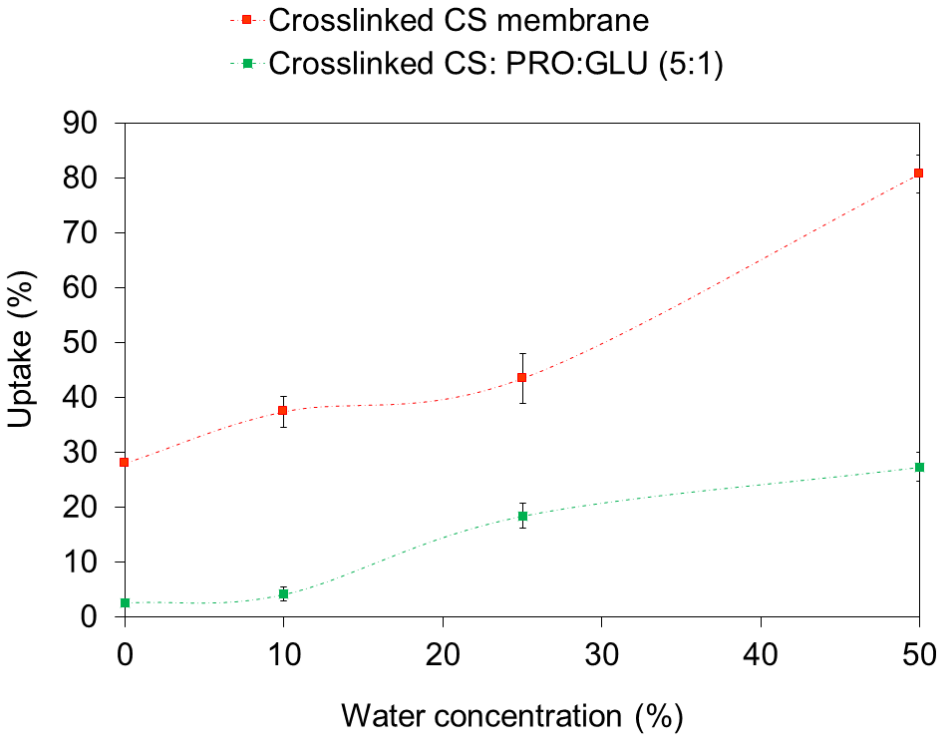

450

451 **Figure 8.** Solvent pptake of CS-eutectic solvent membranes under various water
452 percentage in ethanol (at room temperature). The semi continuous loops are only
453 guiding.

454

455 *3.3.2. PV data comparability of cross-linked CS: PRO:GLU membranes with other*
456 *studies*

457 As for PV testing, it is obvious that the PV separation efficiency of both hybrid and
458 polymer materials is primarily dependent on distinct factors, such as membrane
459 properties (e.g., material type, physiochemical and intrinsic properties, structure, etc.),
460 along with operating parameters including feed composition, operating temperature,

pressure gradient, etc. [34]. Especially, the membrane structure is somehow dictated by the applied membrane preparation strategy [65], while most PV evaluation of membranes has been experimented at different feed concentration and operating parameters. This makes particularly tough to give a fairer comparability among pervaporation results from various works [66]. In our research, we eventually make a comparison of performance outcomes among distinct membrane concepts either unmodified polymer, blends, composites or inorganic tested under close operational parameters, as reported in **Table 2.** Here, the outstanding selectivity, expressed as separation factor, for crosslinked CS:PRO:GLU membrane was found at 20 ºC (approximately 1,427), which represents almost 2-folds bigger α value in comparison to unmodified crosslinked chitosan. In addition to this, the highest permeation rates were acquired at the highest tested temperature (at 50 ºC) in both membranes while showing a decrement in selectivity. The membrane containing the DES showed a slight improvement in permeation (see **Table S1**). When compared with other reports, crosslinked CS:PRO:GLU membranes exhibited better selectivity than other composite membranes, such as crosslinked PVA-filled GO, CS-filled H-ZSM-5, polyimide (PI)-filled ZIF-8, CS-filled titanium dioxide (TiO_2), PI-filled MSS-1, crosslinked PVA-filled ZIF-8-NH_2, among others (see **Table 2**). Depending on the used inorganic fillers filled into the polymer membranes, the aforementioned composites can offer higher permeation rates than our findings. Unfortunately, crosslinked CS:PRO:GLU membranes did not overcome the exceptional selectivity of crosslinked sodium alginate-filled beta zeolite and NaP1 zeolite membranes with unprecedented separation factor values. It is worth pointing out that these membranes (i.e., crosslinked CS:PRO:GLU) are overcoming the

484 selective-permeable trade-off of the pristine CS membranes.

485

Table 2. Comparison of crosslinked CS: PRO: GLU membrane performance with some composites and inorganic membranes tested with similar water-ethanol mixtures.

Membrane concept	Filler content:	Water %	Testing conditions	J (kg m^{-2} h^{-1})	Separation factor	Reference:
Crosslinked CS:PRO:GLU	-	10 wt.%	20 ºC, 1 mbar	0.242	1,425	This work
Crosslinked CS:PRO:GLU		10 wt.%	50 ºC, 1 mbar	0.389	831.7	This work
Crosslinked PVA- GO	1 wt.%	10 wt.%	40 ℃, 3 mbar	0.137	263	[67]
CS-filled H-ZSM-5	8 wt.%	10 wt.%	80 ℃, 10 mbar	0.230	152	[68]
Crosslinked sodium alginate-filled beta zeolite	10 wt.%	10 wt.%	30 ℃, 0.6 mbar	0.130	1,600	[69]
Polyimide-filled ZIF-8	12 wt.%	10 wt.%	42 ℃, 44 mbar	0.260	300	[70]
CS-filled TiO_2	6 wt.%	10 wt.%	80 ℃, 50 mbar	0.340	196	[71]

Polyimide-filled MSS-1	12 wt.%	10 wt.%	42 ℃, 44 mbar	0.310	190	[70]
Crosslinked CS-filled silica	5 wt.%	10 wt.%	70 ℃, 10 mbar	0.410	919	[72]
Crosslinked PVA-filled ZIF-8-NH_2	7.5 wt.%	15 wt.%	40 ℃, 1 mbar	0.120	200	[73]
NaP1 zeolite membranes	-	10 wt.%	75 ºC, 4 mbar	0.45	200 000	[74]
PVA composite membrane	-	10 wt.%	60 ℃, 5 mbar	0.140	170	[75]
PVA composite membrane (PERVAP 2201, Sulzer Chemtech)	-	10 wt.%	60 ℃, 10 mbar	0.100	100	[76]

488

489

3.4. Mass transfer performance

Through the mass transfer model developed for the pervaporation process, and equations 7 and 8, mass transfer resistances can be determined for the different membranes, which are shown in **Table 3**.

Table 3. Mass transfer resistance distribution

		Crosslinked CS			Crosslinked CS:PRO:GLU		
	T (℃)	$R_{liq}\left(\frac{s}{m}\right)\cdot 10^4$	$R_{membrane}\left(\frac{s}{m}\right)$	$R_{overall}\left(\frac{s}{m}\right)\cdot 10^8$	$R_{liq}\left(\frac{s}{m}\right)\cdot 10^4$	$R_{membrane}\left(\frac{s}{m}\right)10^8$	$R_{overal}l\left(\frac{s}{m}\right)\cdot 10^8$
Water	**20**	0.799	0.155	0.155	0.799	0.149	0.149
	30	1,37	0.222	0.222	1,39	0.219	0.219
	40	2,26	0.346	0.346	2,32	0.329	0.329
	50	3,60	0.529	0.529	3,72	0.502	0.502
Ethanol	**20**	1,07	58.3	58.3	1.07	113	113
	30	1,79	64.4	64.4	1.81	132	132
	40	2,90	82.3	82.3	2.96	153	153
	50	4,52	120	120	4.68	209	209

Table 3 shows how the transport stage in the membrane corresponds to the one that presents the greatest resistance to mass transfer for the two membranes under study, as well as for water and ethanol, reaching approximately 99% of the total resistance

distribution of them. On the other hand, despite the great importance of the resistance value to mass transfer of the membrane, differences in behavior can be observed when comparing the same membrane with water and ethanol, at the same temperature. It is seen that in crosslinked CS membrane, the resistance for ethanol transport is two orders of magnitude bigger compared to water, and as for the membrane modified with DES, a difference of 3 orders of magnitude is obtained, which implies that the modification by including DES improves the separation performance, fulfilling the task of obtaining a membrane with a greater hydrophilic character, offering approximately twice the resistance to ethanol than the crosslinked CS membrane, whereas for water, the resistances are similar.

To compare the performance of membrane modification with DES, it is necessary to compare the selectivity factors, this information is presented in **Table 4**.

Table 4. Water/ethanol selectivity for the different membranes.

	Crosslinked CS		Crosslinked CS:PRO:GLU	
T (℃)	$S_{W/E}$	$PSI\ \left(\frac{kg}{m^2h}\right)$	$S_{W/E}$	$PSI\ \left(\frac{kg}{m^2h}\right)$
20	375	87	756	183
30	290	87	600	181
40	238	80	464	163
50	228	85	416	162

Regarding the selectivity factors that both membranes present, it is observed how the incorporation of proline-glucose as DES allows a greater selectivity towards water, mainly because they prevent the passage of ethanol molecules through the membrane, which explains the increase in the resistance of the membrane to ethanol doubling its value respect to the resistance towards ethanol in the Crosslinked CS membrane. The addition of PRO:GLU DES to the membrane allows the PSI of the membrane to improve more than double in comparison with the crosslinked CS membrane, even the membrane performance is greater than that reported in the literature for the water-ethanol system [67].

Finally, the increase in temperature results in selectivity decrement of the Crosslinked CS:PRO:GLU membrane, being the temperature at 20°C the one that presents the best performance, which is corroborated by the PSI value presented by the membrane.

4. Conclusions and future research

This research reveals the fabrication and characterization, for the first time, of dense crosslinked CS-hydrophilic protonated-L-proline: glucose. The membranes present a compelling miscible properties and integration of the original hydrophilic eutectic mixture (PRO:GLU) along the organic biopolymer interface. In general, it was utilized eco-friendly items (including biopolymer, water as primary solvent, “green” eutectic mixture), making the developed hybrid materials as good candidates for fabricating sustainable and eco-friendly dense membranes.

For water-ethanol pervaporation separation, these hybrid membranes offer a 2-fold improved pervaporation yield than the DES-free crosslinked chitosan and slight enhancement in permeation. As a perspective, the forthcoming research must be emphasized on enhancing the permeation yield and membranes’ selective properties when incorporating inorganic phases like nanomaterials. By smartly selecting the hydrophilic nanostructured materials (such as graphene oxide, MXene, UiO-66 MOF), the resultant mixed matrix membranes based on CS may offer unprecedent permeation rates while improving the selective properties as well [23,67]. Also, these membranes can be assayed in other attractive PV separation applications, such as methanol/MTBE [77], water/isopropanol [78], water/hydrazine hydrate [79], requiring hydrophilic membranes. Due to their interesting capability to form H-bonding intermolecular forces, DESs could foster an outperforming extraction of some other polar solvents present in azeotropic systems [17,43]. Variety of available DESs, as well as high potential for new developments in this field, tries to design new DES-based membranes having tailored selectivity. Lately, visualizing a possible preparation protocol in a more sustainable way,

the crosslinker agent (i.e., glutaraldehyde) could be substituted by another less harmful substance. Here, green substances, such as cinnamaldehyde [80], genipin [81], could be an alternative.

Acknowledgments

The authors gratefully acknowledge the financial support from the National Science Centre, Warsaw, Poland – decision no. UMO-2018/30/E/ST8/00642. Financial support from Polish National Agency for Academic Exchange (NAWA) under Ulam Programme (Agreement No. PPN/ULM/2020/1/00005/U/00001) is gratefully acknowledged. R. Castro-Muñoz also acknowledges the School of Engineering and Science and the FEMSA-Biotechnology Center at Tecnológico de Monterrey for their support through the Bioprocess (0020209I13) Focus Group.

Conflict of Interest

The authors declare no conflict of interest.

References

[1] E.L. Smith, A.P. Abbott, K.S. Ryder, Deep Eutectic Solvents (DESs) and Their Applications, Chem. Rev. 114 (2014) 11060–11082. https://doi.org/10.1021/cr300162p.

[2] P. Liu, J.W. Hao, L.P. Mo, Z.H. Zhang, Recent advances in the application of deep eutectic solvents as sustainable media as well as catalysts in organic reactions, RSC Adv. 5 (2015) 48675–48704. https://doi.org/10.1039/c5ra05746a.

[3] J. Huang, X. Guo, T. Xu, L. Fan, X. Zhou, S. Wu, Ionic deep eutectic solvents for the extraction and separation of natural products, J. Chromatogr. A. 1598 (2019) 1–19. https://doi.org/10.1016/j.chroma.2019.03.046.

[4] A.R. Harifi-Mood, F. Mohammadpour, G. Boczkaj, Solvent dependency of carbon dioxide Henry's constant in aqueous solutions of choline chloride-ethylene glycol based deep eutectic solvent, J. Mol. Liq. 319 (2020) 114173. https://doi.org/10.1016/j.molliq.2020.114173.

[5] P. Makoś, G. Boczkaj, Deep eutectic solvents based highly efficient extractive desulfurization of fuels – Eco-friendly approach, J. Mol. Liq. 296 (2019) 111916. https://doi.org/10.1016/j.molliq.2019.111916.

[6] M. Momotko, J. Łuczak, A. Przyjazny, G. Boczkaj, First deep eutectic solvent-based (DES) stationary phase for gas chromatography and future perspectives for DES application in separation techniques, J. Chromatogr. A. 1635 (2020) 461701. https://doi.org/10.1016/j.chroma.2020.461701.

[7] F. Merza, A. Fawzy, I. AlNashef, S. Al-Zuhair, H. Taher, Effectiveness of using deep eutectic solvents as an alternative to conventional solvents in enzymatic biodiesel production from waste oils, Energy Reports. 4 (2018) 77–83. https://doi.org/10.1016/j.egyr.2018.01.005.

[8] Y.P. Mbous, M. Hayyan, A. Hayyan, W.F. Wong, M.A. Hashim, C.Y. Looi, Applications of deep eutectic solvents in biotechnology and bioengineering—Promises and challenges, Biotechnol. Adv. 35 (2017) 105–134. https://doi.org/10.1016/j.biotechadv.2016.11.006.

[9] A.E. Ünlü, A. Arlkaya, S. Takaç, Use of deep eutectic solvents as catalyst: A mini-

603 review, Green Process. Synth. 8 (2019) 355–372. https://doi.org/10.1515/gps-
604 2019-0003.
605 [10] R. Castro-Muñoz, F. Galiano, A. Figoli, G. Boczkaj, Deep eutectic solvents – A
606 new platform in membrane fabrication and membrane-assisted technologies, J.
607 Environ. Chem. Eng. (2021).
608 https://doi.org/https://doi.org/10.1016/j.jece.2021.106414.
609 [11] M. Taghizadeh, A. Taghizadeh, V. Vatanpour, M.R. Ganjali, M.R. Saeb, Deep
610 eutectic solvents in membrane science and technology: Fundamental,
611 preparation, application, and future perspective, Sep. Purif. Technol. 258 (2021)
612 118015. https://doi.org/10.1016/j.seppur.2020.118015.
613 [12] B. Jiang, H. Dou, L. Zhang, B. Wang, Y. Sun, H. Yang, Z. Huang, H. Bi, Novel
614 supported liquid membranes based on deep eutectic solvents for olefin-paraffin
615 separation via facilitated transport, J. Memb. Sci. 536 (2017) 123–132.
616 https://doi.org/10.1016/j.memsci.2017.05.004.
617 [13] Z. Dai, H. Aboukeila, L. Ansaloni, J. Deng, M. Giacinti Baschetti, L. Deng,
618 Nafion/PEG hybrid membrane for CO 2 separation: Effect of PEG on membrane
619 micro-structure and performance, Sep. Purif. Technol. 214 (2019) 67–77.
620 https://doi.org/10.1016/j.seppur.2018.03.062.
621 [14] Z. Dai, L. Ansaloni, J.J. Ryan, R.J. Spontak, L. Deng, Nafion/IL hybrid
622 membranes with tuned nanostructure for enhanced CO2 separation: Effects of
623 ionic liquid and water vapor, Green Chem. 20 (2018) 1391–1404.
624 https://doi.org/10.1039/c7gc03727a.
625 [15] N.M. Mahmoodi, M. Taghizadeh, A. Taghizadeh, Activated carbon/metal-organic

framework composite as a bio-based novel green adsorbent: Preparation and mathematical pollutant removal modeling, J. Mol. Liq. 277 (2019) 310–322. https://doi.org/10.1016/j.molliq.2018.12.050.

[16] B. Jiang, N. Zhang, L. Zhang, Y. Sun, Z. Huang, B. Wang, H. Dou, H. Guan, Enhanced separation performance of PES ultrafiltration membranes by imidazole-based deep eutectic solvents as novel functional additives, J. Memb. Sci. 564 (2018) 247–258. https://doi.org/10.1016/j.memsci.2018.07.034.

[17] R. Castro-Muñoz, A. Msahel, F. Galiano, M. Serocki, J. Ryl, S. Ben Hamouda, A. Hafiane, G. Boczkaj, A. Figoli, Towards azeotropic MeOH-MTBE separation using pervaporation chitosan-based deep eutectic solvent membranes, Sep. Purif. Technol. 281 (2022) 119979. https://doi.org/10.1016/j.seppur.2021.119979.

[18] R. Castro-Muñoz, F. Galiano, V. Fíla, E. Drioli, A. Figoli, Mixed matrix membranes (MMMs) for ethanol purification through pervaporation: Current state of the art, Rev. Chem. Eng. 35 (2019) 565–590. https://doi.org/10.1515/revce-2017-0115.

[19] R. Castro-Muñoz, J. González-Valdez, M.Z. Ahmad, High-performance pervaporation chitosan-based membranes: new insights and perspectives, Rev. Chem. Eng. (2020) 20190051. https://doi.org/https://doi.org/10.1515/revce-2019-0051.

[20] R. Castro-Muñoz, Breakthroughs on tailoring pervaporation membranes for water desalination: A review, Water Res. 187 (2020) 116428. https://doi.org/10.1016/j.watres.2020.116428.

[21] R. Castro-Muñoz, J. González-Valdez, New trends in biopolymer-based membranes for pervaporation, Molecules. 24 (2019).

https://doi.org/10.3390/molecules24193584.

[22] F. Galiano, K. Briceño, T. Marino, A. Molino, K.V. Christensen, A. Figoli, Advances in biopolymer-based membrane preparation and applications, J. Memb. Sci. 564 (2018) 562–586. https://doi.org/10.1016/j.memsci.2018.07.059.

[23] R. Castro-Munõz, MXene : A two-dimensional material in selective water separation via pervaporation, Arab. J. Chem. 15 (2022) 103524. https://doi.org/10.1016/j.arabjc.2021.103524.

[24] R. Castro-Muñoz, A. Cruz-Cruz, Y. Alfaro-Sommers, L.X. Aranda-Jarillo, E. Gontarek-Castro, Reviewing the recent developments of using graphene-based nanosized materials in membrane separations, Crit. Rev. Environ. Sci. Technol. 0 (2021) 1–38. https://doi.org/10.1080/10643389.2021.1918509.

[25] F. Galiano, A. Figoli, R. Castro-mu, Recent advances in pervaporation hollow fiber membranes for dehydration of organics, Chem. Eng. Res. Des. 4 (2020) 68–85. https://doi.org/10.1016/j.cherd.2020.09.028.

[26] P. Janicka, A. Przyjazny, G. Boczkaj, Novel “acid tuned” deep eutectic solvents based on protonated L-proline, J. Mol. Liq. 333 (2021) 115965. https://doi.org/10.1016/j.molliq.2021.115965.

[27] C. Casado-Coterillo, A. Fernández-Barquín, B. Zornoza, C. Téllez, J. Coronas, Á. Irabien, Synthesis and characterisation of MOF/ionic liquid/chitosan mixed matrix membranes for CO2/N2 separation, RSC Adv. 5 (2015) 102350–102361. https://doi.org/10.1039/c5ra19331a.

[28] P.G. Ingole, N.R. Thakare, K. Kim, H.C. Bajaj, K. Singh, H. Lee, Preparation, characterization and performance evaluation of separation of alcohol using

crosslinked membrane materials, New J. Chem. 37 (2013) 4018–4024. https://doi.org/10.1039/c3nj00952a.

[29] K. Ollik, J. Karczewski, M. Lieder, Effect of functionalization of reduced graphene oxide coatings with nitrogen and sulfur groups on their anti-corrosion properties, Materials (Basel). 14 (2021). https://doi.org/10.3390/ma14061410.

[30] N. Oe, N. Hosono, T. Uemura, Revisiting molecular adsorption: unconventional uptake of polymer chains from solution into sub-nanoporous media, Chem. Sci. (2021). https://doi.org/10.1039/d1sc03770f.

[31] D.A. Blackadder, P.I. Vincent, Solvent uptake as a tool for investigating polymer morphology, Polymer (Guildf). 15 (1974) 2–4. https://doi.org/10.1016/0032-3861(74)90065-2.

[32] S. Zereshki, A. Figoli, S.S. Madaeni, S. Simone, M. Esmailinezhad, E. Drioli, Pervaporation separation of MeOH / MTBE mixtures with modified PEEK membrane : Effect of operating conditions, J. Memb. Sci. 371 (2011) 1–9. https://doi.org/10.1016/j.memsci.2010.11.068.

[33] R. Castro-Muñoz, F. Galiano, V. Fíla, E. Drioli, A. Figoli, Matrimid ® 5218 dense membrane for the separation of azeotropic MeOH- MTBE mixtures by pervaporation, Sep. Purif. Technol. 199 (2018) 27–36. https://doi.org/10.1016/j.seppur.2018.01.045.

[34] R.W. Baker, J.G. Wijmans, Y. Huang, Permeability, permeance and selectivity: A preferred way of reporting pervaporation performance data, J. Memb. Sci. 348 (2010) 346–352. https://doi.org/10.1016/j.memsci.2009.11.022.

[35] C. Arregoitia-Sarabia, D. González-Revuelta, M. Fallanza, D. Gorri, I. Ortiz,

695 Polymer inclusion membranes containing ionic liquids for the recovery of n-
696 butanol from ABE solutions by pervaporation, Sep. Purif. Technol. 248 (2020)
697 117101. https://doi.org/10.1016/j.seppur.2020.117101.
698 [36] V. Garcia, N. Diban, D. Gorri, R. Keiski, A. Urtiaga, I. Ortiz, Separation and
699 concentration of bilberry impact aroma compound from dilute model solution by
700 pervaporation, J. Chem. Technol. Biotechnol. 82 (2008) 973–982.
701 https://doi.org/10.1002/jctb.
702 [37] A.I. Johnson, C. -J Huang, Mass transfer studies in an agitated vessel, AIChE J. 2
703 (1956) 412–419. https://doi.org/10.1002/aic.690020322.
704 [38] E.P. Favvas, A. Figoli, R. Castro-Muñoz, V. Fíla, X. He, Polymeric membrane
705 materials for CO2 separations, 2018. https://doi.org/10.1016/B978-0-12-813645-
706 4.00001-5.
707 [39] H.G. Premakshi, K. Ramesh, M.Y. Kariduraganavar, Modification of crosslinked
708 chitosan membrane using NaY zeolite for pervaporation separation of water-
709 isopropanol mixtures, Chem. Eng. Res. Des. 94 (2015) 32–43.
710 https://doi.org/10.1016/j.cherd.2014.11.014.
711 [40] M. Loloei, M. Omidkhah, A. Moghadassi, A.E. Amooghin, Preparation and
712 characterization of Matrimid® 5218 based binary and ternary mixed matrix
713 membranes for CO2 separation, Int. J. Greenh. Gas Control. 39 (2015) 225–235.
714 https://doi.org/http://dx.doi.org/10.1016/j.ijggc.2015.04.016.
715 [41] R. Castro-Muñoz, V. Fíla, M.Z. Ahmad, Enhancing the CO 2 Separation
716 Performance of Matrimid 5218 Membranes for CO 2 /CH 4 Binary Mixtures,
717 Chem. Eng. Technol. 42 (2019) 645–654.

https://doi.org/10.1002/ceat.201800111.

[42] B. Jiang, N. Zhang, B. Wang, N. Yang, Z. Huang, H. Yang, Z. Shu, Deep eutectic solvent as novel additive for PES membrane with improved performance, Sep. Purif. Technol. 194 (2018) 239–248. https://doi.org/10.1016/j.seppur.2017.11.036.

[43] M.K. Hadj-Kali, H.F. Hizaddin, I. Wazeer, L. El blidi, S. Mulyono, M.A. Hashim, Liquid-liquid separation of azeotropic mixtures of ethanol/alkanes using deep eutectic solvents: COSMO-RS prediction and experimental validation, Fluid Phase Equilib. 448 (2017) 105–115. https://doi.org/10.1016/j.fluid.2017.05.021.

[44] J. Serna-Vázquez, M.Z. Ahmad, G. Boczkaj, R. Castro-Muñoz, Latest Insights on Novel Deep Eutectic Solvents (DES) for Sustainable Extraction of Phenolic Compounds from Natural Sources, Molecules. 26 (2021) 5037. https://doi.org/10.3390/molecules26165037.

[45] I.M. Arcana, B. Bundjali, I. Yudistira, B. Jariah, L. Sukria, Study on properties of polymer blends from polypropylene with polycaprolactone and their biodegradability, Polym. J. 39 (2007) 1337–1344. https://doi.org/10.1295/polymj.PJ2006250.

[46] R. Castro-Muñoz, M.Z. Ahmad, V. Fíla, Tuning of Nano-Based Materials for Embedding Into Low-Permeability Polyimides for a Featured Gas Separation, Front. Chem. 7 (2020) 1–14. https://doi.org/10.3389/fchem.2019.00897.

[47] E. Jakubowska, M. Gierszewska, J. Nowaczyk, E. Olewnik-Kruszkowska, Physicochemical and storage properties of chitosan-based films plasticized with deep eutectic solvent, Food Hydrocoll. 108 (2020) 106007. https://doi.org/10.1016/j.foodhyd.2020.106007.

741 [48] M. Khajavian, V. Vatanpour, R. Castro-Muñoz, G. Boczkaj, Chitin and derivative
742 chitosan-based structures — Preparation strategies aided by deep eutectic
743 solvents: A review, Carbohydr. Polym. 275 (2022) 118702.
744 https://doi.org/10.1016/j.carbpol.2021.118702.
745 [49] J.R. Rodríguez-Núñez, T.J. Madera-Santana, D.I. Sánchez-Machado, J. López-
746 Cervantes, H. Soto Valdez, Chitosan/Hydrophilic Plasticizer-Based Films:
747 Preparation, Physicochemical and Antimicrobial Properties, J. Polym. Environ. 22
748 (2014) 41–51. https://doi.org/10.1007/s10924-013-0621-z.
749 [50] H.S. Tsai, Y.Z. Wang, Properties of hydrophilic chitosan network membranes by
750 introducing binary crosslink agents, Polym. Bull. 60 (2008) 103–113.
751 https://doi.org/10.1007/s00289-007-0846-x.
752 [51] Q. Zhang, K. De Oliveira Vigier, S. Royer, F. Jérôme, Deep eutectic solvents:
753 Syntheses, properties and applications, Chem. Soc. Rev. 41 (2012) 7108–7146.
754 https://doi.org/10.1039/c2cs35178a.
755 [52] A.C. Galvis-Sánchez, M.C.R. Castro, K. Biernacki, M.P. Gonçalves, H.K.S.
756 Souza, Natural deep eutectic solvents as green plasticizers for chitosan
757 thermoplastic production with controlled/desired mechanical and barrier
758 properties, Food Hydrocoll. 82 (2018) 478–489.
759 https://doi.org/10.1016/j.foodhyd.2018.04.026.
760 [53] J.Z. Knaul, S.M. Hudson, K.A.M. Creber, Crosslinking of chitosan fibers with
761 dialdehydes: Proposal of a new reaction mechanism, J. Polym. Sci. Part B Polym.
762 Phys. 37 (1999) 1079–1094. https://doi.org/10.1002/(SICI)1099-
763 0488(19990601)37:11<1079::AID-POLB4>3.0.CO;2-O.

764 [54] R.S. Vieira, M.M. Beppu, Interaction of natural and crosslinked chitosan
765 membranes with Hg(II) ions, Colloids Surfaces A Physicochem. Eng. Asp. 279
766 (2006) 196–207. https://doi.org/10.1016/j.colsurfa.2006.01.026.
767 [55] W.Y. Wong, C.Y. Wong, W. Rashmi, M. Khalid, Choline chloride:Urea-based
768 deep eutectic solvent as additive to proton conducting chitosan films, J. Eng. Sci.
769 Technol. 13 (2018) 2995–3006.
770 [56] S.P. Dharupaneedi, R. V. Anjanapura, J.M. Han, T.M. Aminabhavi, Functionalized
771 graphene sheets embedded in chitosan nanocomposite membranes for ethanol
772 and isopropanol dehydration via pervaporation, Ind. Eng. Chem. Res. 53 (2014)
773 14474–14484. https://doi.org/10.1021/ie502751h.
774 [57] M. Kong, X.G. Chen, K. Xing, H.J. Park, Antimicrobial properties of chitosan and
775 mode of action: A state of the art review, Int. J. Food Microbiol. 144 (2010) 51–63.
776 https://doi.org/10.1016/j.ijfoodmicro.2010.09.012.
777 [58] M. Mathaba, M.O. Daramola, Effect of chitosan's degree of deacetylation on the
778 performance of pes membrane infused with chitosan during amd treatment,
779 Membranes (Basel). 10 (2020). https://doi.org/10.3390/membranes10030052.
780 [59] C. Nagel, K. Günther-Schade, D. Fritsch, T. Strunskus, F. Faupel, Free volume
781 and transport properties in highly selective polymer membranes, Macromolecules.
782 35 (2002) 2071–2077. https://doi.org/10.1021/ma011028d.
783 [60] C.M.R. Almeida, J.M.C.S. Magalhães, H.K.S. Souza, M.P. Gonçalves, The role of
784 choline chloride-based deep eutectic solvent and curcumin on chitosan films
785 properties, Food Hydrocoll. 81 (2018) 456–466.
786 https://doi.org/10.1016/j.foodhyd.2018.03.025.

787 [61] A. Pandey, R. Rai, M. Pal, S. Pandey, How polar are choline chloride-based deep
788 eutectic solvents?, Phys. Chem. Chem. Phys. 16 (2014) 1559–1568.
789 https://doi.org/10.1039/c3cp53456a.
790 [62] R. Huang, C. Yeom, Pervaporation separation of aqueous mixtures using
791 crosslinked poly(vinyl alcohol)(pva). II. Permeation of ethanol-water mixtures, J.
792 Memb. Sci. 51 (1990) 273–292.
793 [63] O.A.O. Alshammari, G.A.A. Almulgabsagher, K.S. Ryder, A.P. Abbott, Effect of
794 solute polarity on extraction efficiency using deep eutectic solvents, Green Chem.
795 23 (2021) 5097–5105. https://doi.org/10.1039/d1gc01747k.
796 [64] Y.L. Xue, J. Huang, C.H. Lau, B. Cao, P. Li, Tailoring the molecular structure of
797 crosslinked polymers for pervaporation desalination, Nat. Commun. 11 (2020)
798 1461. https://doi.org/10.1038/s41467-020-15038-w.
799 [65] M. Rezakazemi, A. Ebadi Amooghin, M.M. Montazer-Rahmati, A.F. Ismail, T.
800 Matsuura, State-of-the-art membrane based CO2 separation using mixed matrix
801 membranes (MMMs): An overview on current status and future directions, Prog.
802 Polym. Sci. 39 (2014) 817–861.
803 https://doi.org/10.1016/j.progpolymsci.2014.01.003.
804 [66] A. Figoli, S. Santoro, F. Galiano, A. Basile, Pervaporation membranes:
805 preparation, characterization, and application, in: A. Basile, A. Figoli, M. Khayet
806 (Eds.), Pervaporation, Vap. Permeat. Membr. Distill., First edit, Elsevier Ltd.,
807 Cambridge UK, 2015: pp. 281–304.
808 [67] R. Castro-Muñoz, J. Buera-Gonzalez, O. de la Iglesia, F. Galiano, V. Fíla, M.
809 Malankowska, C. Rubio, A. Figoli, C. Tellez, J. Coronas, Towards the dehydration

of ethanol using pervaporation cross-linked poly(vinyl alcohol)/graphene oxide membranes, J. Memb. Sci. 582 (2019) 423–434. https://doi.org/https://doi.org/10.1016/j.memsci.2019.03.076.

[68] H. Sun, L. Lu, X. Chen, Z. Jiang, Pervaporation dehydration of aqueous ethanol solution using H-ZSM-5 filled chitosan membranes, Sep. Purif. Technol. 58 (2008) 429–436. https://doi.org/10.1016/j.seppur.2007.09.012.

[69] S.G. Adoor, L.S. Manjeshwar, S.D. Bhat, T.M. Aminabhavi, Aluminum-rich zeolite beta incorporated sodium alginate mixed matrix membranes for pervaporation dehydration and esterification of ethanol and acetic acid, J. Memb. Sci. 318 (2008) 233–246. https://doi.org/10.1016/j.memsci.2008.02.043.

[70] A. Kudasheva, S. Sorribas, B. Zornoza, C. Téllez, J. Coronas, Pervaporation of water/ethanol mixtures through polyimide based mixed matrix membranes containing ZIF-8, ordered mesoporous silica and ZIF-8-silica core-shell spheres, J. Chem. Technol. Biotechnol. 90 (2015) 669–677. https://doi.org/10.1002/jctb.4352.

[71] D. Yang, J. Li, Z. Jiang, L. Lu, X. Chen, Chitosan/TiO2 nanocomposite pervaporation membranes for ethanol dehydration, Chem. Eng. Sci. 64 (2009) 3130–3137. https://doi.org/10.1016/j.ces.2009.03.042.

[72] Y.L. Liu, C.Y. Hsu, Y.H. Su, J.Y. Lai, Chitosan-silica complex membranes from sulfonic acid functionalized silica nanoparticles for pervaporation dehydration of ethanol-water solutions, Biomacromolecules. 6 (2005) 368–373. https://doi.org/10.1021/bm049531w.

[73] H. Zhang, Y. Wang, Poly(vinyl alcohol)/ZIF-8-NH2 Mixed Matrix Membranes for

Ethanol Dehydration via Pervaporation, AIChE J. 62 (2016) 1728–1739. https://doi.org/DOI 10.1002/aic.

[74] J.C. Guo, C. Zou, C.Y. Chiang, T.A. Chang, J.J. Chen, L.C. Lin, D.Y. Kang, NaP1 zeolite membranes with high selectivity for water-alcohol pervaporation, J. Memb. Sci. 639 (2021) 119762. https://doi.org/10.1016/j.memsci.2021.119762.

[75] M.S. Schehlmann, E. Wiedemann, R.N. Lichtenthaler, Pervaporation and vapor permeation at the azeotropic point or in the vicinity of the LLE boundary phases of organic/aqueous mixtures, J. Memb. Sci. 107 (1995) 277–282. https://doi.org/10.1016/0376-7388(95)00142-6.

[76] D. Van Baelen, B. Van Der Bruggen, K. Van Den Dungen, J. Degreve, C. Vandecasteele, Pervaporation of water-alcohol mixtures and acetic acid-water mixtures, Chem. Eng. Sci. 60 (2005) 1583–1590. https://doi.org/10.1016/j.ces.2004.10.030.

[77] R. Castro-Muñoz, F. Galiano, Ó. de la Iglesia, V. Fíla, C. Téllez, J. Coronas, A. Figoli, Graphene oxide – Filled polyimide membranes in pervaporative separation of azeotropic methanol–MTBE mixtures, Sep. Purif. Technol. 224 (2019) 265–272. https://doi.org/10.1016/j.seppur.2019.05.034.

[78] H.A. Tsai, Y.S. Ciou, C.C. Hu, K.R. Lee, D.G. Yu, J.Y. Lai, Heat-treatment effect on the morphology and pervaporation performances of asymmetric PAN hollow fiber membranes, J. Memb. Sci. 255 (2005) 33–47. https://doi.org/10.1016/j.memsci.2004.09.052.

[79] R. Castro-Muñoz, G. Boczkaj, Pervaporation Zeolite-Based Composite Membranes for Solvent Separations, Molecules. 26 (2021) 1242.

856 [80] Z. Qin, X. Jia, Q. Liu, B. Kong, H. Wang, Enhancing physical properties of
857 chitosan / pullulan electrospinning nano fi bers via green crosslinking strategies,
858 Carbohydr. Polym. 247 (2020) 116734.
859 https://doi.org/10.1016/j.carbpol.2020.116734.
860 [81] R.A.A. Muzzarelli, Genipin-crosslinked chitosan hydrogels as biomedical and
861 pharmaceutical aids, Carbohydr. Polym. 77 (2009) 1–9.
862 https://doi.org/10.1016/j.carbpol.2009.01.016.
863